Scientific paper

In Situ Durability Characteristics of New and Old Concrete Structures

Guido Frenzer[1], Frank Jacobs[2] and Roberto J. Torrent[3*]

Received 26 May 2020, accepted 17 December 2020 doi:10.3151/jact.19.53

Abstract

This paper analyzes field experimental data obtained on about 30 concrete structures, both new (age up to 1 year) and old (age up to 60 years). The data include *in situ* non-destructive tests (NDT) of air-permeability *kT*, electrical resistivity ρ and surface moisture *m*, as well as tests conducted on drilled cores: O_2-permeability *kO*, water sorptivity a_{24}, MIP, carbonation rate K_c and chloride content *Cl* at 10 to 20 mm depth. The main conclusions are that *in situ kT* of new structures is a good indicator of both *kO* and a_{24}. Regarding old structures, high values of *kT* and *kO* are accompanied by low a_{24} values and by tight MIP pore structure. This phenomenon is attributed to microcracks, with strong effect on permeation but not so much on capillary suction. Similarly, high values of *kT* are not always accompanied by deep carbonation depths. The chloride content did not show correlation with either *kT* or ρ. In situ measurements of ρ, under the testing conditions, did not correlate with any other durability test. Finally, the spread of *kT* values for old structures is significantly wider than for young structures, suggesting that age improves durable concrete but weathering and damage impair non-durable concrete.

1. Introduction

Since 1990, the Swiss Federal Highway Administration (ASTRA) has been funding research projects aimed at studying the durability performance of new and old concrete structures by means of site testing (Torrent and Ebensperger 1993; Torrent and Frenzer 1995; Brühwiler *et al*. 2005; Jacobs 2006; Jacobs *et al*. 2009). The origin of these studies was an article (Menn 1987) written by one of the greatest Swiss bridge designers, late Prof. Christian Menn, asking for R&D projects oriented to reduce bridges maintenance costs by ensuring a better quality of their construction and maintenance. Top of the list of R&D topics proposed was 'Characteristics and Measurement of the Permeability of the Cover Concrete', preferably by non-destructive test (NDT) methods.

One positive result of such research efforts has been the introduction into the Swiss Standards of the need to check the 'tightness' of the cover concrete, or "*Covercrete*" (Newman 1987), on newly-built real structures (SIA 2013). For that purpose, a non-destructive test method, developed in the 90's (Torrent 1992), to measure the coefficient of air-permeability of the *Covercrete* on site was standardized in 2003, updated in 2008 and more recently in 2019 as Annex E of SIA 262/1 (SIA 2019).

A second positive result was the collection of a significant amount of test results, obtained from several structures, both new and old, predominantly built in Switzerland.

In parallel, a large amount of data on pore structure, transport properties and durability tests (e.g. carbonation and chloride ingress), produced by many researchers in investigations made in the laboratory, typically on cast specimens, were compiled in state-of-the-art reports (RILEM 1995, 2007, 2015). However, it is well known that the quality of such specimens, designated as "*Labcrete*" (Newman 1987), is not representative of that achieved in the structure ("*Realcrete*") and, more specifically, of that of the surface layers (*Covercrete*), strongly affected by the applied concreting practices (compaction, finishing, curing), by interaction with the environment and by microcracks. To have a more realistic picture of the quality of the *Covercrete* of real structures, vital for their durability, it is imperative to conduct site tests, which are more laborious, expensive and not always facilitated by the contractors or owners of the structures. These factors explain the relative scarcity of such site data. Yet, a comprehensive survey of several concrete structures in Japan was presented in (Imamoto *et al*. 2014), with data on site air-permeability and carbonation rate; in Switzerland, the air-permeability of some old bridges was also investigated (Adey *et al*. 1998).

The objective of this paper is to present and discuss the experimental results collected from comprehensive site tests conducted on several concrete structures, both new and old. The paper focuses on the relation between non-destructive site tests and several durability tests performed on cores drilled from the tested areas. The test results were obtained and reported by the authors at HMB (Holderbank Management u. Beratung AG, later Holcim Technology Ltd.) and at TFB (Technik und Forschung im Betonbau AG), both in Switzerland (Torrent and Frenzer 1995; Jacobs 2006). They had never been thoroughly and jointly analyzed in the past.

The authors believe that this comprehensive study

[1]Plant Manager, Marti AG Solothurn, CH-3380 Walliswil bei Niederbipp, Switzerland.
[2]Senior Consultant, TFB AG, CH-5013 Wildegg, Switzerland.
[3]Technical Director, Materials Advanced Services Ltd., C1425ABV, Buenos Aires, Argentina. *Corresponding author, *E-mail*: torrent.concrete@gmail.com

provides valuable information on the usefulness and limitations of site testing, on the levels of quality that can be achieved in new structures and how and why this quality can change after decades of service. This information could be useful as well to those involved in the probabilistic modelling of service life of reinforced concrete structures.

2. Structures investigated

The data reported in this paper were collected on a large number of new and old structures. The sample of investigated structures comprise: 17 new structures (with ages at the time of testing between 18 and about 400 days) and 12 older structures (with ages at the time of testing between 17 and 60 years). The results of the investigations conducted by HMB and TFB were reported by Torrent and Frenzer (1995) and Jacobs (2006), respectively.

2.1 New structures

The two structures investigated by HMB were Bözberg highway Tunnel and Schaffhausen Bridge over the Rhine River (Torrent 1999). In both cases, tests were conducted on laboratory slabs (360 × 250 × 120 mm), cast with fresh concrete samples taken from trucks sent to the jobsite and, in parallel, in situ, in the areas where the same batches were placed. In the case of the bridge, as core drilling was forbidden, 1 m cubes were cast and kept close to the real elements they represented, to be sent to HMB laboratory for testing. In Bözberg Tunnel, a single mix was tested (OPC concrete, cube strength at 28 days = 50.5 MPa), whilst in Schaffhausen Bridge, two mixes were tested. One of them, used for the Deck was made with OPC and had a 28-day cube compressive strength of 51.1 MPa; the other, used for the Pylon, was made with a cement containing 8% Silica Fume having a 28-day cube compressive strength of 79.6 MPa.

The 15 structures investigated by TFB consist of five motorway bridges, four buildings for housing and industrial use, five motorway tunnels and one sport football stadium. The investigated elements of the bridges and tunnels consist of concrete with the exposure classes XC4, XD3 and XF4 according to the Swiss Standard (SN EN 206 2013) (w/c ≤ 0.45). The investigated elements of the buildings and the stadium consist of concrete with the exposure classes XC1 according to the Swiss Standard (SN EN 206 2013) (w/c around 0.50). All concretes had a maximum grain size of 32 mm. The cements used are identified in **Table A.3** with a superscript varying from 0 to 5, corresponding to the following types and classes (EN 197-1 classes shown in brackets):

0: not available
1: OPC (CEM I)
2: OPC (CEM I) + Fly-ash
3: Limestone Filler Cement (CEM II/A-LL) + Fly Ash
4: Limestone Filler Cement (CEM II/A-LL)
5: Cement containing Silica Fume (CEM II/A-D)

2.2 Old structures

The three old structures investigated by HMB correspond to bridges. Two bridges are located along Motorway N1 (today A1), linking the cities of Zürich and Bern, near the towns of Oensingen (where the underside of the deck was investigated) and of Rothrist (where the walls of Underpass Z64 were investigated). The third bridge is the Gärtnerstrasse Bridge, in the city of Basel, over the Wiese River (where the underside of the deck was investigated, but also its upper side, after removal of the asphalt overlay during maintenance operations).

The eight structures investigated by TFB correspond to one retaining wall along a motorway, four motorway bridges, two motorway tunnels and one building for housing. The concrete compositions are not known. At the time of construction usually OPC with a w/c ratio less than 0.50 (motorway structures) and approx. 0.60 (inner walls for building) and a maximum grain size of 32 mm were used.

3. Tests performed on the structures

3.1 *In situ* non-destructive tests (NDTs)

The following NDT methods were applied directly on the surface of the structural elements, typically without any previous preparation.

(a) Air-permeability kT (m²), (Torrent test method) described in Annex E of Swiss Standard (SIA 2019); the first version of the standard was issued in 2003.
(b) Surface electrical resistivity ρ (kΩ.cm), (Wenner test method), guidelines in (Polder 2000). Both kT and ρ were measured using the Torrent Permeability Tester instrument (Proceq). It is worth mentioning that ρ was measured with the intention of assessing the moisture conditions of the surface at the moment of measuring kT; hence, both properties were measured at the prevailing temperature and moisture conditions at the moment of test, without any effort to artificially wet or dry the surface.
(c) Surface moisture content m (%), electrical impedance method, using a Tramex Concrete Encounter device.

3.2 Semi-destructive tests applied on drilled cores

The following tests were applied in the laboratory, on drilled cores saw-cut to size:

(a) O_2-permeability kO (m²), according to the RILEM-Cembureau test method (RILEM 1999), measured on Ø100 × 50 mm discs, conditioned by 6 days oven drying at 50°C, followed by 1-day cooling to 20°C in a desiccator. The reported value is the average of the results obtained under relative applied pressures of 0.5 and 2.5 bar.
(b) Water sorptivity a_{24} (g/m²/s^{½}), HMB procedure, was obtained by placing the same discs used for kO in contact with 3 mm of water and monitoring the mass increase due to capillary suction, along the lines of Annex A of the Swiss Standard SIA 262/1 (SIA 2019).

The mass of water absorbed per unit surface area of the specimen (g/m²), after 24 hours of contact, divided by the square root of 24 hours ($s^{½}$) is the water sorptivity a_{24}.

(c) Water sorptivity a_{24} (g/m²/$s^{½}$), TFB reported values, was obtained on Ø50 × 50 mm discs, conditioned by 2 days oven drying at 50°C, followed by 1-day cooling to 20°C in a desiccator. The values originally reported were of the so-called "Water conductivity" q_w (g/m²/h), after Annex A of Swiss Standard SIA 262/1 (SIA 2019). For comparison with HMB results, the q_w values were converted into a_{24} values through Eq. (1), developed at TFB from regression analysis of many test data:

$$a_{24} = 3.4 + 1.142\,(q_w - 2.26) \quad (1)$$

where q_w in (g/m²/h) and a_{24} in (g/m²/$s^{½}$).

(d) Pore characteristics, from MIP analysis of diamond-cut small specimens, about 10 × 20 × 40 mm each, that could fit into the MIP analyser (Carlo Erba Series 2000 WS with macropore unit 120), capable of measuring pore radii between 3.7 and 300 000 nm. The samples were saw-cut from the exposed surface so as to penetrate 40 mm into the *Covercrete*, with all surfaces open to Hg intrusion. Four individual samples were tested for MIP from each tested surface. The reported values are the total porosity V_t (%) (median of the four values indicated by the instrument) and a 'mean' pore radius r_p (nm) (median of the four values indicated by the instrument). The reported values of r_p are close to the threshold pore radius, calculated as the peak of the derivative of intruded volume with the logarithm of pore radius.

(e) Carbonation rate K_c (mm/$y^{½}$), based on the measurement of the carbonation depth X_c (mm) by the phenolphthalein method, on freshly exposed surfaces of cores drilled from old structures, divided by the square root of the age (years) of the structure.

(f) Chloride content *Cl* (% of cement weight), obtained by titration analysis of a 10 mm-thick slice saw-cut at 10 to 20 mm from the surface of a drilled core.

(g) Compressive strength f'_c in MPa, measured on Ø100 × 100 mm cores drilled from old structures.

The reported compressive strength results for new structures correspond to tests on 120 or 150 mm cubes, moist-cured during 28 days (f'_{c28}).

4. Experimental results

4.1 New structures

Tables A.1 and **A.2** of the Annex present the test results obtained by HMB in Bözberg Tunnel and Schaffhausen Bridge, respectively, whilst **Table A.3** presents the test results obtained by TFB in the 15 structures they investigated. To be remarked is that HMB results correspond to individual measurements made *in situ* or on cores drilled from the same location, whilst TFB results are statistical values, calculated from several individual values obtained for each element.

Except for *kT*, the central values reported are the averages of the individual values obtained (e.g. ρ_{avg} and m_{avg} for electrical resistivity and surface moisture, respectively) and the scatter is their standard deviation (e.g. s_ρ for resistivity).

Regarding air-permeability *kT*, that is best represented by a log-normal distribution (Conciatori 2005; Denarié *et al*. 2005; Jacobs and Hunkeler 2006; Misák *et al*. 2008), the central value is given by kT_{gm}, which is the geometric mean of the individual *kT* values and the scatter by s_{LOG}, that is the standard deviation of the $\log_{10}$ of the individual *kT* values (Jacobs 2006).

4.2 Old structures

Tables A.4 to **A.6** of the Annex present the test results obtained by HMB on Oensingen Bridge (30 years old), Underpass Z64 (20 years) and Gärtnerstrasse Bridge in Basel (60 years), respectively. **Table A.7** presents the results obtained by TFB in the 8 structures investigated. It was not possible to identify the cement type used in the old structures investigated, hence all are identified by the code "0" as per the classification in Section 2.1. Most likely, these structures were built with OPC, strongly predominant in Switzerland by the time of their construction.

4.3 Laboratory results

Test results obtained on laboratory cast specimens kept 21 days in a dry room (20°C, 50% RH) after 0, 7, or 28 days moist curing, reported in Tables 3.1-III and 3.2-IV of the study by Torrent and Ebensperger (1993) and in Tables 1.2.1.1, 1.2.1.2 and 3.2.1.1 of that by Torrent and Frenzer (1995), are often included in the analysis of the site data, as reference.

It is worth mentioning that interesting laboratory and site test results of MIP parameters (threshold pore radius and total pore volume) have been reported (Sakai *et al*. 2013, 2014), showing close relationships between them and both *kT* and water permeability. Another attempt to relate air-permeability and carbonation with the microstructure of cement paste (investigated by SEM-EDX) was reported by Jeon *et al*. (2012).

5. Analysis of the results

The figures included in this chapter refer to N (New Structures) and O (Old Structures), followed by a number between 0 and 5, corresponding to the cement type classification presented in Section 4.1. The data for new structures were taken from Tables A.1 to A.3 and for the Old Structures from Tables A.4 to A.6, indicated in some legends.

5.1 Relation *in situ* tests vs. strength

Figure 1 presents the relation between the *in situ* coefficient of air-permeability *kT* and cube compressive strength f'_{c28} of new structures and core compressive

strength f'_c of old structures. The dashed line represents the relation between gas permeability K_g and cube compressive strength f'_{c28cyl} converted from cylinder strength using the conversion by L'Hermite (1997), which is Eq. 5.1-123 in *fib* Model Code 2010 (*fib* 2012). This equation is meant for tests on laboratory samples. **Figure 2** is similar but for *in situ* electrical resistivity ρ in abscissae.

Figure 1 shows that the results obtained on new structures do not depart significantly from the fib predictions (dotted line), although some results show, for the same strength, higher *kT* values than the predicted ones. This may reflect the loss of quality of the cover concrete (evaluated *in situ* by *kT*), compared with that obtained on laboratory specimens, something noticeable in **Tables A.1** and **A.2** and discussed by Torrent (1999).

Regarding old structures, the first aspect to remark from **Fig**. **1** is the relatively high core strengths obtained (values typically between 40 and 100 MPa). However, these high strengths are not always accompanied by equally low permeability *kT*, the points departing even farther from the *fib* prediction dotted line. Indeed, high permeabilities ($kT > 1.0 \times 10^{-16}$ m²) were measured on old structures, even when the core strength f'_c was in the range 40 to 75 MPa. As discussed later, this is attributed to deterioration of the *Covercrete* due to weathering, applied loads and, often, to microcracking.

Yet, an expected trend of higher site *kT* for lower core strength f'_c can be observed for old structures in **Fig. 1**, not so evident for new structures; the difference is that, in the former, the core strength reflects better the quality of the in-place concrete than the cast cubes.

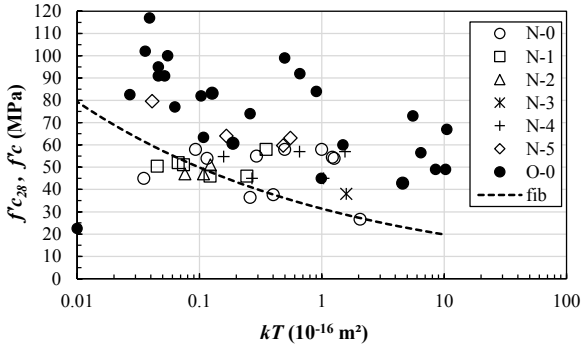

Fig. 1 Relation between site air permeability *kT* and compressive strength.

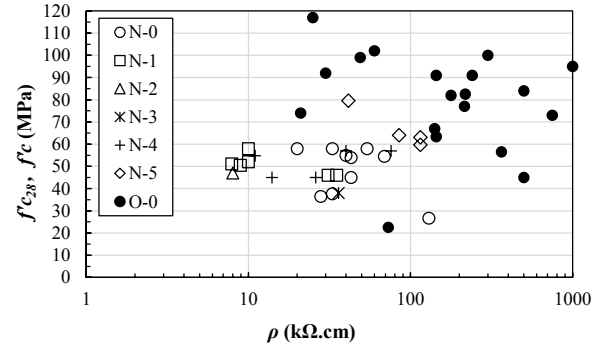

Fig. 2 Relation between site electrical resistivity ρ and compressive strength.

Figure 2 shows that no clear relationship exists between f'_{c28} and ρ, tested on site. One reason for the missing trend is, that, in new structures a large variety of cement types was used and the cement type influences resistivity much more than strength. For instance, three out of the four structures built with a silica fume-containing cement (diamond symbols) show high values of ρ, confirming the effect silica fume has in raising the electrical resistivity. RILEM recommendations (Polder 2000) indicate that the electrical resistivity of concretes made with blast furnace slag (> 65% slag) or fly ash (> 25%) or silica fume (> 5%) is about 5 times higher than for those made with OPC. In the case of **Fig. 2**, the expected trend of higher site resistivity ρ for higher core strength f'_c cannot be observed.

The relation between electrical resistivity and compressive strength was studied by Ramezanianpour *et al*. (2011) in a comprehensive laboratory investigation involving 57 mixes made with nine different binders. The correlation was very good ($R^2 = 0.87$ approx.) when applied to mixes made with the same binder, but turned rather poor ($R^2 = 0.41$) when all binders were included.

In the case of **Fig. 2**, the results shown correspond to field data of both strength and ρ. It is therefore important to have in mind the many factors that can influence the ρ readings, on top of that of the cement type, already discussed. One of the most comprehensive analysis of these factors was made by Azarsa and Gupta (2017), identifying w/c ratio, temperature and moisture of the concrete, vicinity of rebars and the presence of cracks as important factors influencing the results. To those factors, Thomas *et al*. (2013) add the pore structure and the composition of the pore solution (related to the cement type and w/c ratio), carbonation and contamination with chlorides. The effect of temperature was studied by Coyle *et al*. (2016) who reported that ρ is reduced by factor of 3 when the temperature increases from 5 to 30°C. The strong effect of moisture and moisture gradients on ρ was thoroughly investigated by Minagawa *et al*. (2017), whilst the role of reinforcement on ρ was dealt with by Angst and Elsener (2014) and by Salehi *et al*. (2016). Improving the conditions for site measurement of the electrical resistivity ρ as, for instance, by trying to saturate the concrete surface, is far from easy Presuel-Moreno *et al*. (2010).

This myriad of factors affecting field test results of ρ can explain the recorded lack of correlation in **Fig. 2**.

5.2 Relation between *in situ* tests

Figure 3 presents the relation between air-permeability *kT* and electrical resistivity ρ, both measured on site on new and old structures, at the temperature and moisture conditions prevailing at the moment of test. It can be seen that both variables show no dependence from each other, contrary to the expected decreasing relation of ρ with increasing *kT*. Here again, the factors discussed in connection with **Figs. 1** and **2**, apply.

5.3 Relation between *in situ* and laboratory tests

Figures 4 to 7 present the relation between the air-permeability *kT* and *kO*, a_{24}, r_p and V_t, respectively, for new and old structures. *kT* was measured on site and the other four properties on samples cut from cores drilled from the same locations. The Annex tables containing the data are indicated. As reference, the values obtained in the laboratory, under the conditions described in Section 4.3, are also plotted.

Figure 4 shows that the coefficient of air-permeability *kT*, measured *in situ* on new and old structures, correlate reasonably well with the coefficient of O_2-permeability *kO*, measured in the lab on preconditioned cores drilled (at the same place) from the same structures. Most interesting, the relation obtained on new and old structures fits quite well to that obtained on specimens, cast, cured, preconditioned and tested in the laboratory. It is worth remarking that the *kT* values obtained on Oensingen bridge (O-A.4) span five orders of magnitude. The scatter can be explained by the different degrees of saturation and different volumes of *Covercrete* investigated, *kT* exploring a Ø50 mm cylinder of variable length (typically between 5 and 100 mm, depending on the permeability) whilst *kO* explores a Ø150 mm × 50 mm thick cylinder.

Figure 5 shows a rather different picture. The water sorptivity a_{24} of new structures is significantly higher, for the same *in situ kT*, than that obtained on old structures; moreover, the results on new structures fit quite well the relation obtained on laboratory specimens. The water sorptivity a_{24} of old structures is less than half the value obtained on laboratory specimens for the same *kT*, especially noticeably for *kT* values above 0.1×10^{-16} m². The following effects can contribute to this phenomenon: a) the carbonation of old structures has a stronger effect on the capillary suction than on gas-permeability; b) high permeability values of *kT* in old structures, after years of weathering, are due to the appearance of microcracks in the ITZ and/or matrix, that have a stronger effect on gas permeability than on capillary suction; c) the different penetration of the tests into the *Covercrete* and d) some possible effect of moisture on *kT*, eliminated by oven-drying for a_{24}.

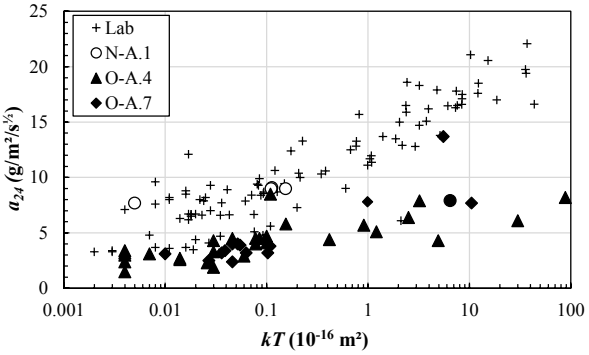

Fig. 5 Relation between site air-permeability *kT* and lab water sorptivity a_2.

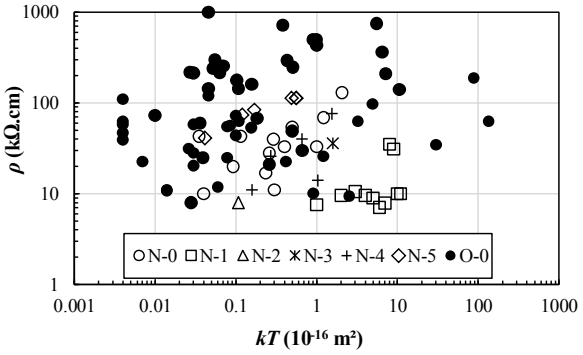

Fig. 3 Relation between resistivity ρ and air-permeability *kT* for new and old structures.

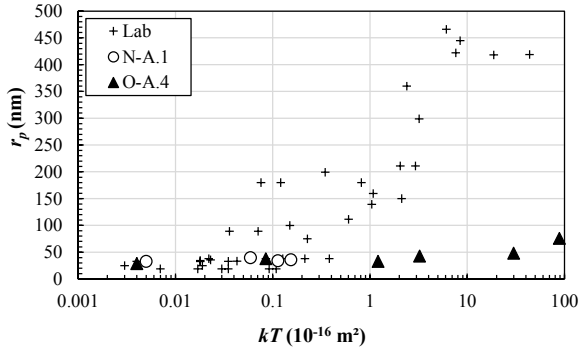

Fig. 6 Relation between site air-permeability *kT* and pore radius r_p.

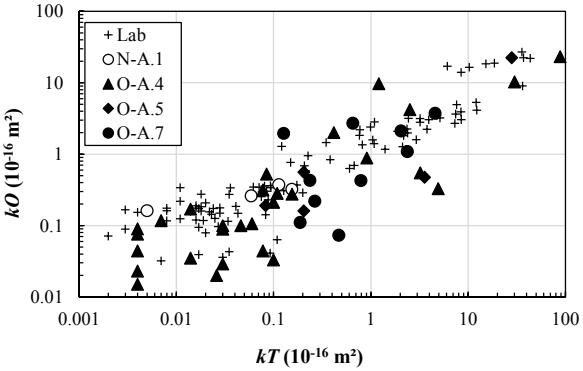

Fig. 4 Relation between site air-permeability *kT* and lab O_2-permeability *kO*.

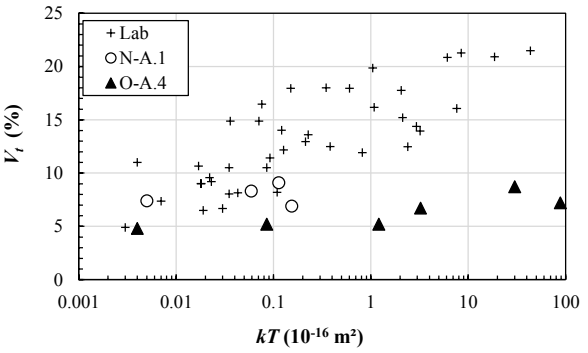

Fig. 7 Relation between site air-permeability *kT* and total pore volume V_t.

Figures 6 and **7** throw some light on the previous discussion. They present the relation of kT with mean pore radius r_p and with total porosity V_t, respectively, for new and old structures. Results obtained on laboratory specimens are also included for reference purposes. It can be seen that the pore structure (determined by MIP) of old concretes of permeability kT above 0.1×10^{-16} m² is much tighter (lower radius r_p and total porosity V_t) than what would be expected from testing laboratory specimens. Since the MIP test results plotted in **Figs. 6** and **7** correspond to the non-carbonated zone, the effect of carbonation has to be excluded. Actually, as expected, the pore structure of the carbonated zone is even tighter, see few MIP results in Table A.4.

Figures 8 and **9** also help in the clarification of the above discussion. They show the relation between the water sorptivity a_{24} and the mean pore radius r_p and total porosity V_t, respectively, for few new and old structures, as well as for laboratory tests on cast specimens. We can see that, contrary to the relation kT vs pore structure (**Figs. 6** and **7**), the a_{24} results obtained on the new and old structures fit quite well to those obtained on laboratory specimens.

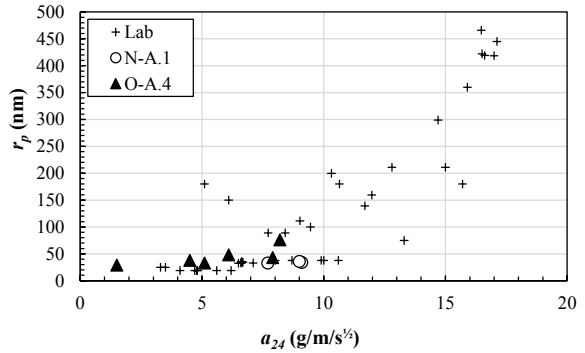

Fig. 8 Relation between water sorptivity a_{24} and pore radius r_p.

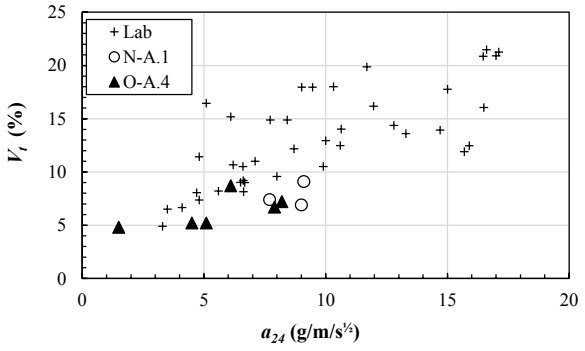

Fig. 9 Relation between water sorptivity a_{24} and total pore volume V_t.

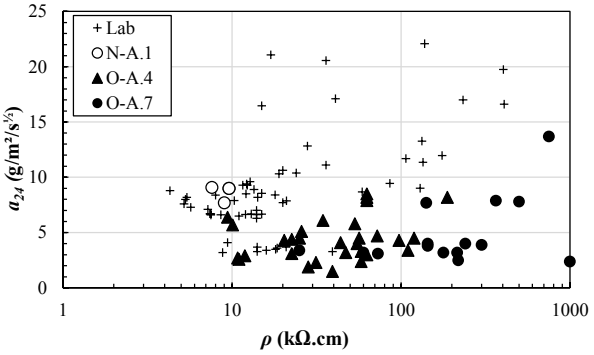

Fig. 10 Relation between water sorptivity a_{24} and electrical resistivity ρ.

The analysis of the data presented in **Figs. 5** to **9** indicates that the microstructure of the concrete in the old structures remains quite tight (low r_p and V_t values) after decades of exposure to the mildly severe Swiss climate (that yet includes frost-thaw cycles and de-icing salts for bridges and tunnels). The very high air- and O_2- permeabilities (kT and kO) of the old concretes can then be attributed to defects (bond or matrix microcracks) that facilitate the flow of gas under pressure, but that do not influence so much capillary suction (relatively low a_{24}).

No clear relation was found between the electrical resistivity ρ and microstructural (r_p and V_t) or transport parameters (a_{24} and kO), same as shown in **Fig. 3** with site permeability kT. For the sake of brevity, just the relation between a_{24} and ρ is shown in **Fig. 10**, where the expected trend of higher a_{24} for lower ρ is not apparent. Since the main focus of the investigations here reported was on air-permeability kT testing, the conditions under which the electrical resistivity ρ was measured (avoiding rainy or wet weather, variable temperatures, vicinity of steel) were not ideal for the latter. Additionally, resistivity is more strongly influenced by the cement type than the pore size distribution. This was the reason, too, to prescribe in the Swiss Standard SIA 262/1 (SIA 2019) the measurement of the surface moisture m by an electrical impedance-based instrument, abandoned the resistivity as originally recommended (Torrent and Frenzer 1995; Jacobs *et al*. 2009).

5.4 Relation between *in situ* tests and durability performance of old structures

As described in Section 3.2, in several old concrete structures, the carbonation rate K_c was determined and, in some of them, also the chloride content Cl in a 10 to 20 mm deep slice, cut from drilled cores. **Figure 11** presents the relation of K_c with the site measurement of kT (the white triangles correspond to Basel bridge deck that was covered with asphalt in service which, logically, yielded $K_c = 0$).

Figure 11 shows a trend observed also in structures tested in Japan and Portugal (Imamoto *et al*. 2016), of which use was made to assess the service life of Port of Miami Tunnel (Torrent *et al*. 2013). It indicates that, for very low kT values (below 0.01×10^{-16} m²), the carbonation rate K_c is negligible and that, for low kT values (between 0.01×10^{-16} m² and 0.1×10^{-16} m²) K_c is rather low (typically below 2.0 mm/y^{½}). For higher kT values there is some uncertainty on the carbonation rate that was treated mathematically by Neves *et al*. (2018). This may be due to the already discussed presence of weathering

microcracks that have a larger effect on kT than on K_c, as already suggested by Imamoto *et al*. (2016).

Regarding chloride content *Cl*, no clear relation can be observed with either site air-permeability kT (**Fig. 12**) or with site electrical resistivity ρ (**Fig. 13**). This can be due to the fact that the chloride content near the surface depends not only on the transport properties of the *Covercrete* but also on the vicinity and intensity of the chloride sources. The penetration (by mix modes) of chloride ions from salty solutions in permanent or sporadic contact with the structure is very complex, due to the overlapping of several physical mechanisms (Hunkeler 2000). Chlorides may penetrate by permeation, carried by the saline water solution and, alternatively or complementary, by ion diffusion. Rain washout and evaporation, affecting predominantly the surface layers, add complication to the phenomenon.

In a separate investigation (Jacobs 2008) found a relation between kT and the chloride content of 20 to 30 mm deep concrete slices for several columns of six 30 years old bridges crossing a Swiss motorway.

5.5 *In situ kT* tests statistical distributions

Figure 14 shows the frequency distribution of the central value of kT (kT_{gm}) obtained from new and old structures, whilst **Fig. 15** shows the frequency distributions of the scatter of kT values (s_{LOG}). The number of cases analyzed for new and old structures amounts to 35 each.

Although the results were not obtained at young and later ages on exactly the same structures, some patterns can be observed. First, the histogram of kT_{gm} values (**Fig. 14**) of new structures spans 5 class intervals, whilst that of old structures spans 9 class intervals. This may be attributed, a bit speculatively, to a phenomenon by which concrete that is originally of "good" quality (low kT_{gm}) and durable becomes better with the passage of time, whilst concrete that is originally of insufficient quality (high kT_{gm}) impairs after decades of service and weathering exposure.

The same reason can explain why the scatter of kT (s_{LOG}) within each element tested tends to be larger for old structures compared with new structures (**Fig. 15**).

6. Conclusions

Based on the analysis of the experimental results of this

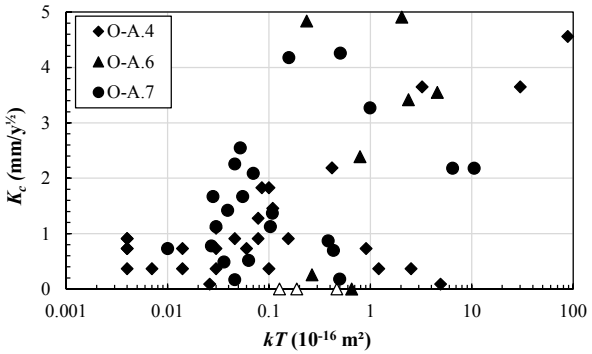

Fig. 11 Relation between air-permeability kT and carbonation rate K_c.

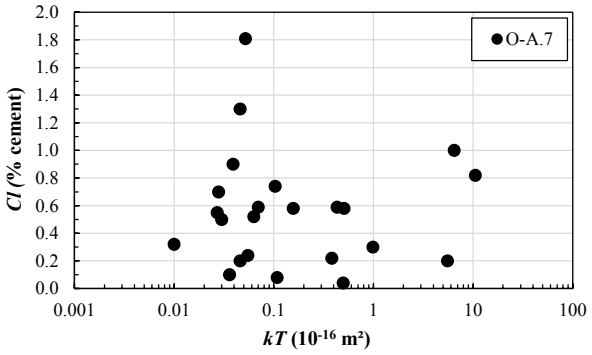

Fig. 12 Relation between air-permeability kT and chloride content in 10 to 20 mm slice.

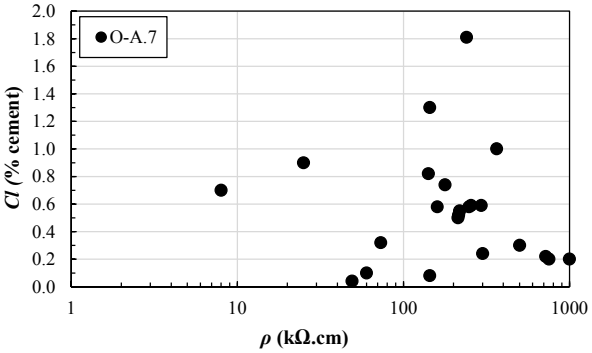

Fig. 13 Relation between resistivity ρ and chloride content in 10 to 20 mm slice.

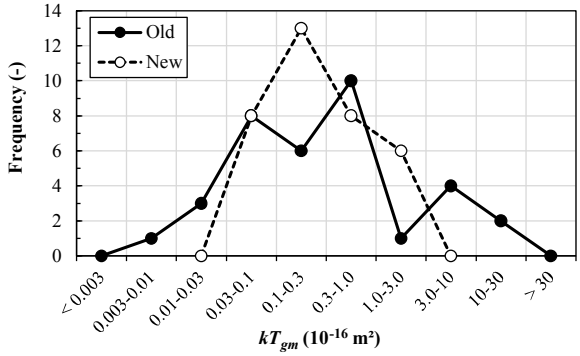

Fig. 14 Frequency distribution of geometric mean of kT for new and old structures.

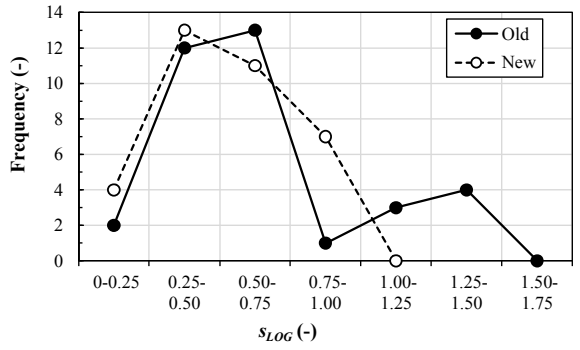

Fig. 15 Frequency distribution of scatter s_{LOG} of kT for new and old structures.

investigation, the following conclusions can be drawn:

(1) The *in situ*, non-destructive measurement of the coefficient of air-permeability *kT*, of new (some months old) and old (several decades) structures, provides a good indication of the gas-permeability of the *Covercrete,* correlating consistently well with O_2-permeability *kO*, measured in the laboratory on companion drilled cores.
(2) Measuring *in situ* the coefficient of air-permeability *kT* of new structures, provides a good indication of the water sorptivity of the material a_{24}, measured in the laboratory on companion drilled cores
(3) Some old structures present high values of *kT* whilst the intrinsic pore structure of the concrete (determined by MIP) is quite tight, which can be attributed to damage (microcracks) after decades of service and weathering
(4) As a result, high values of *kT* in old structures are not always accompanied by proportionally high values of water sorptivity a_{24}, which is believed to be less affected by microcracks
(5) Possibly for a similar reason, high values of *kT* in old structures are not always accompanied by deep carbonation, although here the microclimate (especially moisture of the concrete) plays a significant role on carbonation
(6) The recorded range of (geometric) mean values of *kT* in old structures is much wider than in new structures, suggesting that durable concrete becomes better with time, whilst the non-durable concrete gets worse with decades of service and weathering
(7) Similarly, higher values of the scatter of *kT* (s_{LOG}), within a single structural element, can be found in old structures, compared with new structures
(8) The high variability in the concrete properties measured in old structures constitutes a challenge for modelers, even when applying probabilistic approaches
(9) The results of electrical resistivity show no relation whatsoever with the other durability characteristics, measured *in situ* or in the laboratory. A different picture may have emerged if practical means of compensating external influences had been applied (e.g. testing at similar temperatures, saturating the concrete prior to the test, avoiding neighboring steel bars, etc.)

7. Final remarks

The authors believe that more research efforts should be placed on investigating the characteristics of the concrete in real structures, their spatial variability, and the phenomena involved in their evolution with age, something that is unlikely to be mimicked in the laboratory. This would help in making prediction models (e.g. for carbonation or chloride ingress) more realistic and reliable.

Additionally, quality control through testing specimens cast with the delivered concrete are specified in detail in concrete standards [e.g. SN EN 206 (2013)], but quality control *in situ* by testing the structure is mostly missing. NDTs and/or drilling and investigating cores from new structures are important to evaluate the true permeability and thickness of the *Covercrete*, to reassure the owner that the quality of the end-product required for reaching the design or expected service life of the structure has been achieved. This should be part of the birth-certificate documentation.

References

Adey, B., Roelfstra, G., Hajdin, R. and Brühwiler, E., (1998). "Permeability of existing concrete bridges." In: G. L. Balázs, Ed. *Proc. 2nd International PhD Symposium in Civil Engineering*, Budapest, Hungary 26-28 August 1998. Budapest: Publishing Company of the Technical University of Budapest.

Angst, U. M. and Elsener, B., (2014). "On the applicability of the Wenner method for resistivity measurements of concrete." *ACI Materials Journal*, 111(6), 661-671.

Brühwiler, E., Denarié, E., Wälchli, T., Maître, M. and Conciatori, D., (2005). "*Applicability of Torrent permeability measurement for quality control of cover concrete* (Swiss Federal Roads Office Report No. 587)." Berne: Swiss Federal Roads Office. (in French)

Conciatori, D., (2005). "*Effect of microclimate on the initiation of corrosion of reinforcing steels in reinforced concrete structures*." Thesis (PhD). Federal Polytechnical University of Lausanne. (in French)

Coyle, A., Spragg, R., Amirkhanian, A. and Weiss, J., (2016). "Measuring the influence of temperature on electrical properties of concrete." In: M. Azenha, I. Gabrijel, D. Schlicke, T. Kanstad and O. M. Jensen, Eds. *Proc. International RILEM Conference on Materials, Systems and Structures in Civil Engineering, Segment on Service Life of Cement-Based Materials and Structures*, Lyngby, Denmark 22-24 August 2016. Paris: RILEM Publications SARL, Vol. 1, 211-220.

Denarié, E., Conciatori, D., Maître, M. and Brühwiler, E., (2005). "Air permeability measurements for the assessment of the in situ permeability of cover concrete." In: M. G. Alexander, H. D. Beushausen, F. Dehn and P. Moyo Eds. *Proc. International Conference, ICCRRR-1*, Cape Town, South Africa 21-23 November 2005. Boca Raton, Florida, USA: CRC Press, 180-182.

fib, (2012). "*Final draft of Model Code 2010 for concrete structures* (fib Bulletins 65 and 66)." Lausanne, Switzerland: Fédération Internationale du Béton.

Hunkeler, F., (2000). "Corrosion in reinforced concrete: processes and mechanisms." In: H. Böhni Ed. *Corrosion in Reinforced Concrete Structures*. Cambridge, UK: CRC Press, 1-45.

Imamoto, K., Shimozawa, K., Nagayama, M., Yamasaki, J. and Tanaka, A., (2014). "Relationship between air-permeability and carbonation progress of concrete in Japan." In: D. Bjegović, H. Beushausen and M.

Serdar, Eds. *Proc. RILEM International Workshop on Performance-based Specification and Control of Concrete Durability*, Zagreb, Croatia 11-13 June 2014. Paris: RILEM Publications SARL, 325-333.

Imamoto, K., Neves, R. and Torrent, R., (2016). "Carbonation rate in old structures assessed with air-permeability site NDT." In: *Proc. 8th International Conference on Bridge Maintenance, Safety and Management (IABMAS 2016)*, Foz do Iguaçú, Brazil 26-30 June 2016, 178-184.

Jacobs, F., (2006). "*Air permeability as a parameter for the quality of the concrete cover of concrete structures* (Swiss Federal Roads Office Report No. 604)." Berne: Swiss Federal Roads Office. (in German)

Jacobs, F., (2008). "Non-destructive testing of concrete." *der Bauingenieur (The Civil Engineer)*, 3, 24-27. (in German)

Jacobs, F. and Hunkeler, F., (2006). "Non destructive testing of the concrete cover - Evaluation of permeability test data." *Proc. International RILEM Workshop on Performance Based Evaluation and Indicators for Concrete*. Madrid, Spain 19-21 March 2006. Paris: RILEM Publications SARL, 207-214.

Jacobs, F., Denarié, E., Leemann, A. and Teruzzi T., (2009). "*Recommendations for quality control of concrete with air permeability measurements* (Swiss Federal Roads Office Report No. 641)." Berne: Swiss Federal Roads Office. (in German)

Jeon, J., Kanda, T., Momose, H. and Mihashi, H., (2012). "Development of high-durability concrete with a smart artificial lightweight aggregate." *Journal of Advanced Concrete Technology*, 10(7), 231-239.

L'Hermite, R., (1997). "Current ideas on concrete technology, Part 3: Failure of concrete." In: F. H. Wittmann, Ed. *RILEM: Fifty Years of Evolution of Science and Technology of Building Materials and Structures*. Freiburg, Germany: Aedificatio Publishers, 537-550. (in French)

Menn, C., (1987). "Bridge maintenance research." *Schweizer Ingenieur und Architekt (Swiss Engineers and Architects)*, 43, 1253-1254. (in German)

Minagawa, H., Miyamoto, S. and Hisada, M., (2017). "Relationship of apparent electrical resistivity measured by four-probe method with water content distribution in concrete." *Journal of Advanced Concrete Technology*, 15(6), 278-289.

Misák P., Kucharczyová B. and Vymazal T., (2008). "Evaluation of permeability of concrete by using instrument Torrent" In: *Proc. Juniorstav 2008, the 10th Conference of Post-graduate Students*, Brno, Czech Republic 23 January 2008. Brno: Faculty of Civil Engineering, Brno University of Technology. (in Czech)

Neves, R., Torrent, R. and Imamoto, K., (2018). "Residual service life of carbonated structures based on site non-destructive tests." *Cement and Concrete Research*, 109, 10-18.

Newman, K., (1987). "Labcrete, Realcrete and Hypocrete - Where we can expect the next major durability problems." In: *ACI SP-100 Concrete Durability.* Farmington Hills, Michigan, USA: American Concrete Institute, 2, 1259-1983.

Polder, R., (2000). "Draft recommendation test method for on site measurement of resistivity of concrete." *Materials and Structures*, 33, 603-611.

Presuel-Moreno, F. J., Suares, A. and Liu, Y., (2010). "*Final report - Characterization of new and old concrete structures using surface resistivity measurements*." Florida, USA: Florida Department of Transportation Research Center.

Ramezanianpour, A. A., Pilvar, A., Mahdikhani, M. and Moodi, F., (2011). "Practical evaluation of relationship between concrete resistivity, water penetration, rapid chloride penetration and compressive strength." *Construction and Building Materials*, 25, 2472-2479.

RILEM, (1995). "*Performance criteria for concrete durability* (RILEM Technical Report 12)." London and New York: E & FN Spon.

RILEM, (1999). "*Tests for gas permeability of concrete - Preconditioning of concrete test specimens for the measurement of gas permeability and capillary absorption of water - Measurement of the gas permeability of concrete by the RILEM - Cembureau method* (Recommendation of RILEM TC 116-PCD)." London and New York: E & FN Spon.

RILEM, (2007). "*Non-destructive evaluation of the penetrability and thickness of the concrete cover, State-of-the-art report of RILEM TC 189-NEC* (RILEM Report 40)." Paris: RILEM Publications SARL.

RILEM, (2016). "*Performance-based specifications and control of concrete durability: State-of-the-art report of RILEM TC 230-PSC* (RILEM Report 18)." Dordrecht: Springer Netherlands.

Sakai, Y., Nakamura, C. and Kishi, T., (2013). "Correlation between permeability of concrete and threshold pore size obtained with epoxy-coated sample." *Journal of Advanced Concrete Technology*, 11(13), 189-195.

Sakai, Y., Nakamura, C. and Kishi, T., (2014). "Evaluation of mass transfer resistance of concrete based on representative pore size of permeation resistance." *Construction and Building Materials*, 51, 40-46.

Salehi, M., Ghods, P. and Burkan Isgor, O., (2016). "Numerical investigation of the role of embedded reinforcement mesh on electrical resistivity measurements of concrete using the Wenner probe technique." *Materials & Structures*, 49, 301-316.

SIA, (2013). "*Concrete construction* (Swiss Standard SIA 262)." Zurich, Switzerland: Swiss Society of Engineers and Architects. (in German)

SIA, (2019). "*Concrete construction - Complementary specifications* (Swiss Standard SIA 262/1)." Zurich, Switzerland: Swiss Society of Engineers and Architects. (in German)

SN EN 206, (2013). "*Concrete - Part 1: Specification, properties, manufacture and conformity* (Swiss Standard SN EN 206)". Winterhur, Switzerland: Swiss Association

for Standardization. (in German)

Thomas, M., Moffatt, T., Yi, H. and Smith, D. E., (2013). "Electrical methods for estimating the chloride resistance of concrete." In: *Proc. ACI Fall 2013 Convention*, Phoenix, Arizona, USA 20-24 October 2013.

Torrent, R. J., (1992). "A two-chamber vacuum cell for measuring the coefficient of permeability to air of the concrete cover on site." *Materials & Structures*, 25, 358-365.

Torrent, R., (1999). "The gas-permeability of high-performance concretes: site and laboratory tests." In: *ACI SP-186 High-Performance Concrete Performance and Quality of Concrete Structures.* Farmington Hills, Michigan, USA: American Concrete Institute, 291-308.

Torrent, R. and Ebensperger, L., (1993). "*Study of methods for measuring and assessing the characteristic values of cover concrete on the construction site* (Report No. 506 of the Swiss Federal Roads Office)." Berne: Swiss Federal Roads Office. (in German)

Torrent, R. J. and Frenzer, G., (1995). "*Methods for measuring and assessing the characteristic values of the concrete cover on the construction site - Part II* (Report No. 516 of the Swiss Federal Roads Office)." Berne: Swiss Federal Roads Office. (in German)

Torrent, R., Armaghani, J. and Taibi, Y., (2013). "Evaluation of Port of Miami tunnel segments: Carbonation and service life assessment made using on-site air permeability tests." *Concrete International*, 35(5), 39-46.

Annex

Tables A.1 to A.7 show the test results obtained from the various structures.

Table A.1 Test results obtained by HMB on Bözberg Tunnel.

	Laboratory Tests				Site Tests					
Tested Truck	kT 10^{-16} m²	kO 10^{-16} m²	a_{24} g/m²/s^{½}	ρ kΩ.cm	kT 10^{-16} m²	kO 10^{-16} m²	a_{24} g/m²/s^{½}	ρ kΩ.cm	r_p nm	V_t %
M4	0.028	0.177	9.3	12.3	0.113	0.374	9.1	7.6	34	9.1
M5	0.083	0.142	7.9	11.3	0.154	0.321	9	9.6	36	6.9
M7	0.008	0.161	9.6	12.8	0.059	0.26	---	10.6	40	8.3
M8	0.081	0.357	9.4	12.2	0.111	---	9	9.6	---	---
M9	0.008	0.156	8.4	14.3	0.005	0.161	7.7	9	33	7.4
M10	0.025	0.126	8.2	14.2	0.015	---	---	7.1	---	---
N	6	6	6	6	6	4	4	6		
Central	0.026	0.187	8.8	12.9	0.045	0.279	8.7	8.9		
Scatter	0.45	0.085	0.7	1.2	0.59	0.091	0.7	1.3		

Table A.2 Test results obtained by HMB on Schaffhausen Bridge.

Pylon	**Test Point**	kT 10^{-16} m²	ρ kΩ.cm	kO 10^{-16} m²	a_{24} g/m²/s^{½}	r_p nm	V_t %
Lab	2 slabs	0.002	39.3	0.071	3.3	---	---
Cube 1	1-1	0.027	9.4	0.097	4.1	---	---
	1-2	0.034	8.8	0.115	3.2	---	---
	1-3	0.016	14.1	0.176	3.7	---	---
	1-4	0.008	20.9	0.116	3.7	---	---
Cube 2	2-1	0.003	14.1	0.089	3.3	25	4.9
	2-2	0.011	18.5	0.124	3.6	---	---
	2-3	0.003	16	0.166	3.4	---	---
	2-4	0.019	18.1	0.118	3.5	25	6.5
Cubes 1+2	**N**	9	9	9	9		
	Central	0.009	16.8	0.119	3.5		
	Scatter	0.45	9	0.034	0.3		
On Site	**N**	23	23				
	Central	0.041	41.4				
	Scatter	0.27	16.9				

Deck	**Test Point**	kT 10^{-16} m²	ρ kΩ.cm	kO 10^{-16} m²	a_{24} g/m²/s^{½}	r_p nm	V_t %
Lab	2 slabs	0.017	7.4	0.144	6.7	---	---
Cube 3	3-1	0.011	5.4	0.218	8.2	---	---
	3-2	0.016	4.3	0.189	8.8	---	---
	3-3	0.008	5.2	0.175	7.6	---	---
	3-4	0.02	7.5	0.207	6.7	---	---
Cube 4	4-1	0.004	7.2	0.153	7.1	33	11.0
	4-2	0.035	7.5	0.272	6.6	33	10.5
	4-3	0.011	5.3	0.338	8.0	---	---
	4-4	0.2	5.7	0.288	7.3	---	---
Cubes 3+ 4	**N**	9	9	9	9		
	Central	0.017	6.2	0.22	7.4		
	Scatter	0.48	1.2	0.066	0.8		
On Site	**N**	10	10				
	Central	0.074	7.9				
	Scatter	0.68	0.7				

Table A.3 Test results obtained by TFB on 15 new structures.
(The superscripts varying from 0 to 5 indicate the types and classes of cement used, as explained in Section 2. 1)

Structure	**Elements Tested**	N	kT_{gm}	s_{LOG}	ρ_{avg}	s_{ρ}	m_{avg}	**Age**	$f'c_{28}$
		---	10^{-16} m²	---	kΩ.cm		%	days	MPa
Bridge 1 Box girder[0]	Wall	4	0.093	0.32	20	4	5.6	179	58
	Under. Deck	6	0.497	0.42	54	16	5.1		
	Floor	4	1.00	0.68	33	2	3.9		
Bridge 2 [0]	Underside Deck	8	1.221	0.44	69	6	5.1	162	54.5
Bridge 3 [0] Abutment Wall	Inner Side	6	0.115	0.55	43	11	5.4	246	54
	Outer Side	5	1.261	0.23	---	---	5		
Bridge 4 [1]	Pillar 0-1 m	9	0.122	0.35	35	13	4.3	192	46
	Pillar 1 - 3.4 m	3	0.244	0.47	31	16	4.3		
Bridge 5 Guide Wall	Element 44 [0]	3	0.3	0.22	11	2	---	18	---
	Element 6 [2]	3	0.123	0.30	---	---	---	277	51
	Element 20 [3]	4	1.583	0.35	36	3	---	204	38
	Element 12 [1]	5	0.351	0.61	10	3	---	259	58
Building 1 [4]	Wall Outer Side	20	0.158	0.93	11	3	---	175	54.8
	Wall Inner Side	21	2.062	0.68	130	95	---	153	26.7#
Building 2 [0]	Ceiling	10	0.401	0.76	33	1	---	182	37.7
	Wall	16	0.26	0.76	28	4	---	182	36.5
Building 3 [4]	Wall	15	0.035	0.65	43	18	5.1	136	45
Building 4 [0]	Wall	15	0.292	0.57	40	5	---	1786	55*
Stadium [4]	T-Beam Side A	18	0.269	0.75	26	27	---	286	45
	T-Beam Side B	12	1.035	0.45	14	3	---		
	Walls D, E, F	15	0.659	0.49	40	13	4.5	404	57
	Walls A, B, C	20	1.546	0.59	76	26	4.4		57
Tunnel 2 [1]	Wall	18	0.067	0.77	10		5.6	413	52
Tunnel 3 Wall [2]	w/o microcrack	13	0.076	0.09	---	---	---	22	47
	w/ microcrack	14	0.108	0.56	8	1	---		
Tunnel 4 [1]	Dome	15	0.04	0.89	10	2	> 6.5	---	---
Tunnel 5 [1]	Dome	8	0.234	0.34	17	3	> 6.5	---	---
Tunnel 6 Central Wall [5]	40-41	5	0.118	0.19	75	3	4.4	---	63.1
	1000-1001	6	0.551	0.41	115	3	4	---	59.7
	1995-1996	6	0.554	0.87	115	3	4	---	64
	2598-2599	5	0.485	0.79	115	3	3.8	---	57.8
	3200-3201	5	0.166	0.34	85	3	4.2	---	63.5
		Sets	32	32	29	28	17		
		Min	0.04	0.09	8	1	3.8		# core
		Avg	0.5	0.53	46	10	4.6		* rebound
		Max	2.06	0.93	130	95	>6.5		

Table A.4 Test results obtained by HMB on deck underside of Oensingen Bridge.

Elements Tested	Test #	kT	ρ	kO	a_{24}	K_c	r_p (NC)	r_p (C)	V_t (NC)	V_t (C)
		10^{-16} m²	kΩ.cm	10^{-16} m²	g/m²/s^{½}	mm/y^{½}	nm	nm	%	%
1	1	0.417	22.6	2	4.4	2.19	---	---	---	---
	2	88.49	188.5	23.2	8.2	4.56	76	14	7.2	7.0
	3	30.1	34.5	10.26	6.1	3.65	48	33	8.7	6.2
	4	0.109	62.8	0.281	8.5	1.46	---	---	---	---
2	5	0.004	58.1	0.023	2.4	0.91	---	---	---	---
	6	0.046	119.4	0.099	4.5	0.91	---	---	---	---
	7	0.004	62.8	0.044	3.0	0.91	---	---	---	---
	8	3.23	62.8	0.546	7.9	3.65	43	35	6.7	4.5
3	9	0.085	56.6	0.527	4.5	1.83	38	---	5.2	---
	10	0.004	110	0.09	3.4	0.73	---	---	---	---
	11	0.004	47.1	0.076	3.2	0.73	---	---	---	---
	12	0.03	58.1	0.099	3.3	1.10	---	---	---	---
4	13	0.03	20.4	0.089	4.3	0.73	---	---	---	---
	14	0.014	10.8	0.17	2.7	0.73	---	---	---	---
	15	0.014	11	0.035	2.6	0.37	---	---	---	---
	16	0.007	22.6	0.117	3.1	0.37	---	---	---	---
	17	0.06	11.9	0.106	2.9	0.73	---	---	---	---
	19	0.03	28.3	0.029	1.9	0.37	---	---	---	---
	20	0.004	39.3	0.015	1.5	0.37	29	---	4.8	---
5	22	4.93	97.4	0.328	4.3	0.09	---	---	---	---
6	23	0.91	10.1	0.881	5.7	0.73	---	---	---	---
	24	1.21	25.8	9.667	5.1	0.37	33	---	5.2	---
7	25	0.078	55	0.316	4.0	0.91	---	---	---	---
	26	0.1	44	0.211	4.1	0.37	---	---	---	---
8	27	2.52	9.4	4.196	6.4	0.37	---	---	---	---
	28	134.8	62.8	4.134	8.2	2.74	---	---	---	---
9	29	0.155	53.4	0.275	5.8	0.91	---	---	---	---
	30	0.026	31.4	0.02	2.3	0.09	---	---	---	---
10	31	0.1	72.3	0.033	4.7	1.83	---	---	---	---
	32	0.078	25.1	0.044	4.5	1.28	---	---	---	---
	N	30	30	30	30	30				
	Central	0.128	50.5	1.9	4.5	1.2				
	Scatter	1.28	38.8	4.8	1.9	1.1				

NC: Non-carbonated
C: Carbonated

Table A.5 Test results obtained by HMB on walls of Underpass Z64.

Element Tested	Test Position	kT 10^{-16} m²	kO 10^{-16} m²
Lateral Walls	1	0.205	0.559
	2	0.205	0.16
	3	0.083	0.19
	4	3.57	0.474
	5	28.15	22.35
	N	5	5
	Central	0.811	4.75
	Scatter	1.06	9.84

Table A.6 Test results obtained by HMB on the deck of Basel Bridge.

Elements Tested	Test Position	kT 10^{-16} m²	kO 10^{-16} m²	K_c mm/y^{½}	f'_c MPa
Deck underside	1/u	43.36	---	5.87	---
	3/u	0.266	0.22	0.26	---
	4/u	4.58	3.739	3.55	42.9
	5/u	2.37	1.09	3.42	---
	6/u	0.79	0.426	2.39	---
	7/u	0.236	0.429	4.84	---
	8/u	0.653	2.717	0	---
	9/u	2.04	2.114	4.91	---
Deck top side	1/o	0.188	0.11	0	60.7
	3/o	0.469	0.073	0	---
	5/o	0.127	1.952	0	83.2
	N	11	10	11	
	Central	0.909	1.29	1.94	
	Scatter	0.74	1.28	2.11	

Table A.7 Test results obtained by TFB on 8 old structures.

Structure	Element Tested	N --	kT_{gm} 10^{-16} m²	s_{LOG} ---	ρ kΩ.cm	m %	Age years	f'_c MPa	K_c mm/y^{½}	Cl %	a_{24} g/m²/s^{½}
Retaining Wall	19 (cracked)	6	0.183	1.16	68	4.1		---	---	---	---
	21	6	0.497	0.42	49	5.1	30	99	0.18	0.04	---
	26	6	1	0.68	432	3.9		---	---	---	---
Bridge 10 Abutment	Side A	15	0.039	0.81	25	6.1	36	117	1.42	0.90	3.4
	Side H	7	0.028	0.4	8	6.2		---	1.67	0.70	---
Bridge 11	Pillar 323 B	6	6.456	0.54	364	4.7	33	56.5	2.18	1.00	7.9
	Pillar 318 B	6	0.383	0.62	718	3.7		---	0.87	0.22	---
	Pillar 207 B	6	0.046	0.32	999	3.7		95	0.17	0.20	2.4
	Pillar 205 B	6	0.07	0.53	255	4.0		---	2.09	0.59	---
	Pillar 204 B	7	0.432	1.29	294	4.2		---	0.7	0.59	---
	Pillar 201 B	7	0.506	0.44	248	4.4		---	4.26	0.58	---
	Pillar 201 Z	7	0.027	1.11	218	4.6		82.5	0.78	0.55	2.5
	Pillar 204 Z	6	0.103	0.7	178	4.2		82	1.13	0.74	3.2
	Pillar 205 Z	6	0.157	0.43	160	4.6		---	4.18	0.58	---
	Pillar 207 Z	7	0.063	0.49	215	4.1		77	0.52	0.52	3.2
	Pillar 318 Z	6	0.03	0.39	213	4.6		---	1.13	0.50	---
	Pillar 323 Z	9	10.55	0.7	141	4.7		67	2.18	0.82	7.7
Bridge 12	Pillar	5	0.904	0.65	500	2.8	25	84	---	---	---
	Pylon	5	0.662	1.31	30	4.4		92	---	---	---
	"Sails"	3	0.26	0.59	21	4.4		74	---	---	---
Bridge 13	Wall	5	0.108	0.36	144	4.3	30	63.4	1.37	0.08	3.8
	Underside Deck	5	0.01	0.38	73	3.8		22.5	0.73	0.32	3.1
Tunnel 10	Wall F2	3	0.055	0.42	300	3.1	26	100	1.67	0.24	3.9
	Wall F3	3	0.036	0.52	60	4.0		102	0.49	0.10	3.2
	Wall F5	3	0.046	0.32	144	4.1		91	2.26	1.30	4.0
	Wall F4	3	0.052	0.1	240	3.8		91	2.55	1.81	4.0
Tunnel 11	Block 2	4	7.184	0.68	210	---	17	---	---	---	---
	Block 80	3	0.99	0.13	500	---		45	3.27	0.30	7.8
	Block 413	5	5.549	0.7	750	---		73	5.70	0.20	13.7
Building 10 Slabs over	2nd basem. floor	2	10.293	1.27	---	2.0	22	49	---	---	---
	Ground Floor	5	8.531	0.52	---	2.0		49	---	---	---
	1st basem. floor	3	1.492	0.42	---	2.0		60	---	---	---
	Sets		32	32	29	29					
	Min		0.01	0.10	8	2.0					
	Avg		1.77	0.61	261	4.1					
	Max		10.55	1.31	999	6.2					